

# Effective Temperatures in Athermal Systems Sheared at Fixed Normal Load

Ning Xu<sup>1</sup> and Corey S. O'Hern<sup>1,2</sup>  
<sup>1</sup> *Department of Mechanical Engineering,  
 Yale University, New Haven, CT 06520-8284.*  
<sup>2</sup> *Department of Physics, Yale University,  
 New Haven, CT 06520-8120.*

(Dated: March 23, 2022)

We perform molecular dynamics simulations of repulsive athermal systems sheared at fixed normal load to study the effective temperature  $T_L$  defined from time-dependent fluctuation-dissipation relations for density. We show that these systems possess two distinct regimes as a function of the ratio  $T_S/V$  of the granular temperature to the potential energy per particle. At small  $T_S/V$ , these systems are pressure-controlled and  $T_L$  is set by the normal load. In contrast, they behave as quasi-equilibrium systems with  $T_L \approx T_S$  that increases with shear rate at large  $T_S/V$ . These results point out several problems with using  $T_L$  in thermodynamic descriptions of slowly sheared athermal systems.

PACS numbers: 64.70.Pf, 61.20.Lc, 05.70.Ln, 83.50.Ax

Athermal and glassy systems driven by shear or other external forces are by definition not in thermal equilibrium. Fluctuations in these systems are induced by the driving force and do not arise from random thermal motion. However, there are obvious similarities between equilibrium thermal systems and driven systems that reach a nonequilibrium steady-state. In fact, there have been many attempts to develop thermodynamic and statistical descriptions [1] of these systems including kinetic theories for driven granular gases [2], the Edward's entropy formalism for granular packings [3, 4], and applications of equilibrium linear response and fluctuation-dissipation (FD) relations [5] to define effective temperatures in aging [6, 7] and sheared glasses [8, 9] and compacting [10, 11] and sheared granular materials [12, 13].

The approach that employs FD relations to define effective temperatures in athermal and glassy systems has shown great promise. First, effective temperatures from FD relations for several quantities such as density and pressure have been shown to be the same [8, 14]. Second, FD relations can be applied to dense systems with elastic particles in contrast to other approaches. FD relations can also be measured experimentally in athermal systems such as foams and granular materials. However, it is still not clear whether effective temperatures from FD relations can be used in thermodynamic descriptions of dense shear flows. Many important questions remain unanswered, for example, what variables should be used to construct an equation of state and do effective temperature gradients generate heat flow? We conduct molecular dynamics (MD) simulations of sheared, athermal systems to begin to address these questions.

Nearly all numerical simulations that have measured FD relations in sheared athermal and glassy systems have been performed at constant volume. We will conduct our simulations at constant normal load (or external pressure), instead, and this has several advantages. First, it has been shown that sheared, athermal systems behave

differently in these two ensembles. At constant normal load, these systems can dilate in response to an applied shear stress [15, 16]. We will determine how the ability to dilate affects FD relations and properties of effective temperatures defined from them. Simulations at constant normal load will also enable us to determine whether the effective temperature is more sensitive to changes in pressure or shear stress.

Our principal result is that the effective temperature  $T_L$  defined from FD relations for density is controlled by pressure in slowly-sheared athermal systems. We find that for all shear rates below  $\dot{\gamma}_c$ , the effective temperature is independent of shear rate at fixed normal load. Above  $\dot{\gamma}_c$ ,  $T_L$  increases with shear rate and as  $\dot{\gamma}$  increases further the systems obey quasi-equilibrium FD relations at all times. The characteristic shear rate that separates the pressure-controlled from the quasi-equilibrium regime can be estimated using the ratio of kinetic to potential energy [13]. When the ratio is small, a strong force network exists and the effective temperature is set by the pressure. When kinetic energy dominates, velocity fluctuations are large, which causes frequent rearrangements, diffusion, and quasi-equilibrium behavior.

We now provide the essential details of the MD simulations. The systems contained  $N/2$  large and  $N/2$  small particles with equal mass  $m$  and diameter ratio 1.4 to prevent shear induced ordering and segregation [17]. The particles interacted via one of the following pairwise, purely repulsive potentials:

$$V^S(r_{ij}) = \frac{\epsilon}{\alpha} (1 - r_{ij}/\sigma_{ij})^\alpha \quad (1)$$

$$V^{RLJ}(r_{ij}) = \frac{\epsilon}{72} [(\sigma_{ij}/r_{ij})^{12} - 2(\sigma_{ij}/r_{ij})^6 + 1], \quad (2)$$

where  $\epsilon$  is the characteristic energy scale and  $\sigma_{ij} = (\sigma_i + \sigma_j)/2$  and  $r_{ij}$  are the average diameter and separation of particles  $i$  and  $j$ . The repulsive linear ( $\alpha = 2$ ) and Hertzian ( $\alpha = 5/2$ ) spring potentials (Eq. 1) have been used to model granular materials [18, 19]. In contrast

to Eq. 1, the repulsive Lennard-Jones (RLJ) potential (Eq. 2) has an infinite repulsive core at small  $r_{ij}$ . Both interaction potentials are zero for  $r_{ij} \geq \sigma_{ij}$ .

For athermal dynamics, the position and velocity of each particle in the bulk is obtained by solving

$$m \frac{d^2 \vec{r}_i}{dt^2} = \vec{F}_i^r - b \sum_j (\vec{v}_i - \vec{v}_j), \quad (3)$$

where  $\vec{F}_i^r = -\sum_j dV(r_{ij})/dr_{ij} \hat{r}_{ij}$  is the total repulsive force on particle  $i$ ,  $\vec{v}_i$  is the velocity of particle  $i$ ,  $b > 0$  is the damping constant, and sums over  $j$  only include particles overlapping particle  $i$ . Shear is imposed by moving a rough and disordered top boundary in the  $x$ -direction at fixed speed  $u$ , while a similar bottom wall a distance  $L_y$  away remains stationary.

To sustain a fixed normal load  $P_{ext}$  in the  $y$ -direction, the top boundary was moved rigidly according to

$$M \frac{d^2 L_y}{dt^2} = F_y^w - F_{ext} - b \sum_j \left( \frac{dL_y}{dt} - v_{yj} \right), \quad (4)$$

where  $M$  is the mass of the top wall,  $F_y^w$  is the total repulsive force acting on the top wall from interactions with particles in the bulk, and  $F_{ext} = P_{ext} L_x L_z$  ( $P_{ext} L_x$ ) is the external normal force applied to the top wall in 3d (2d). The equations of motion were solved using a 5th order Gear predictor-corrector integration scheme [20]. After an initial transient at each  $u$  and  $P_{ext}$ , forces in the  $y$ -direction balance on average, the system fluctuates about  $\langle L_y \rangle$ , and a linear shear flow is established with shear rate  $\dot{\gamma} = u/\langle L_y \rangle$ . Relatively small system sizes  $N = 1024$  were studied to inhibit the formation of nonlinear velocity profiles [21]. Periodic boundary conditions were implemented in the  $x$  ( $z$ ) direction. We use  $\sigma$ ,  $\epsilon$ , and  $\sigma/\sqrt{m/\epsilon}$ , where  $\sigma$  is the small particle diameter, as the units of length, energy, and time, respectively. All quantities are expressed in reduced units below.

In equilibrium systems, the fluctuation-dissipation theorem requires that the autocorrelation function of a physical quantity is proportional at *all* times  $t$  to that quantity's response to a small conjugate perturbation, and the proportionality constant gives the temperature. Response and correlation are not proportional at all times in sheared glassy and athermal systems [5]. However, several recent studies of FD relations for density in these systems have shown that they can still be used to define an effective temperature that characterizes shear-induced fluctuations at long-time scales [8, 9]. Similar measurements in 3d sheared athermal systems, but at fixed normal load, are displayed in Fig. 1 (a). We plot the integrated response  $R(t)$  of the density of the large particles at wavevector  $\vec{k} = k_0 \hat{z}$

$$\rho(\vec{k}, t) = \frac{1}{N_L} \sum_{j=1}^{N_L} e^{i\vec{k} \cdot \vec{r}_j(t)} \quad (5)$$

to a spatially modulated force with period  $2\pi/k_0$  applied along  $\vec{k}$  at  $t = 0$  and all subsequent times versus the

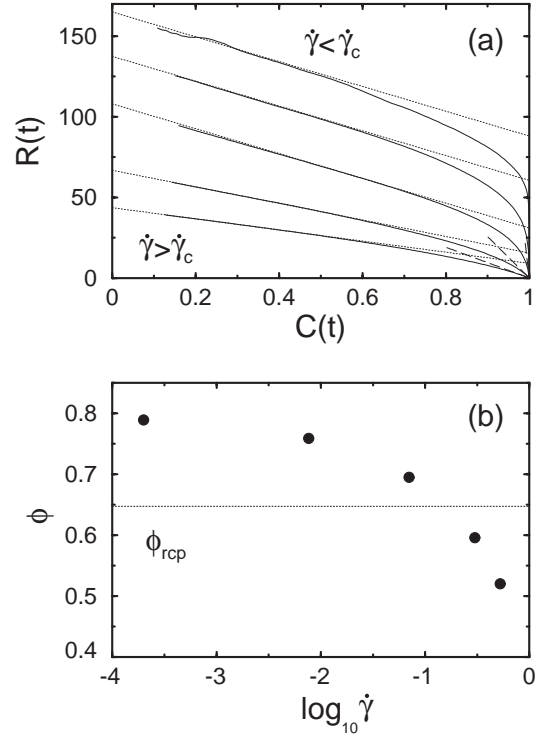


FIG. 1: (a)  $R(t)$  vs.  $C(t)$  (solid lines) for density  $\rho(\vec{k})$  at  $\vec{k} = 9\hat{z}$  for 3d systems with RLJ interactions and  $b = 0.5$  sheared at fixed normal load  $P_{ext} = 0.1$ . The dotted (dashed) lines have slope  $-1/T_L$  ( $-1/T_S$ ). Five shear rates are shown:  $\dot{\gamma} = 0.53, 0.30, 0.07, 7.7 \times 10^{-3}$ , and  $2.0 \times 10^{-4}$  from bottom to top.  $T_L$  is constant for  $\dot{\gamma} < \dot{\gamma}_c \approx 0.2$ . (b) Volume fraction  $\phi$  vs.  $\dot{\gamma}$  for the same systems in (a).  $\phi_{rcp} \approx 0.648$  for 3d bidisperse systems.

density autocorrelation function  $C(t)$  [22]. This figure shows that response versus correlation for  $\rho(\vec{k})$  can be nonlinear at short times in sheared athermal systems. In contrast, the slope of  $R(C)$  is constant at long times, which allows the long-time effective temperature  $T_L$  to be defined as

$$-1/T_L = \left. \frac{dR}{dC} \right|_{C \rightarrow 0}. \quad (6)$$

Previous studies have shown that  $T_L$  does not depend strongly on the magnitude [8] or direction of  $\vec{k}$  [9]. The slope of  $R(C)$  for  $\rho(\vec{k})$  at  $\vec{k} = k_0 \hat{z}$  in the  $t \rightarrow 0$  limit is  $-1/T_S$ , where  $T_S = m\langle v_z^2 \rangle$  is the granular temperature.

In Fig. 1 (a), we show  $R(C)$  for several shear rates at fixed normal load  $P_{ext} = 0.1$ . At low shear rates, the long-time slope of  $R(C)$  is independent of  $\dot{\gamma}$ . However, when  $\dot{\gamma}$  increases above a characteristic shear rate  $\dot{\gamma}_c$ , the long-time slope of  $R(C)$  begins to decrease with increasing  $\dot{\gamma}$ . Thus, at constant normal load,  $T_L$  is constant for  $\dot{\gamma} < \dot{\gamma}_c$ , but increases for  $\dot{\gamma} > \dot{\gamma}_c$ . Fig. 1 (b) shows the variation of the volume fraction  $\phi$  with  $\dot{\gamma}$  for the systems in (a). To compensate for increases in normal force from increases in  $\dot{\gamma}$ , the systems expand in the  $y$ -direction. Fig. 1 (b) emphasizes that effective temperatures depend on the time scale over which they are measured even in systems that are 20% below random close packing.

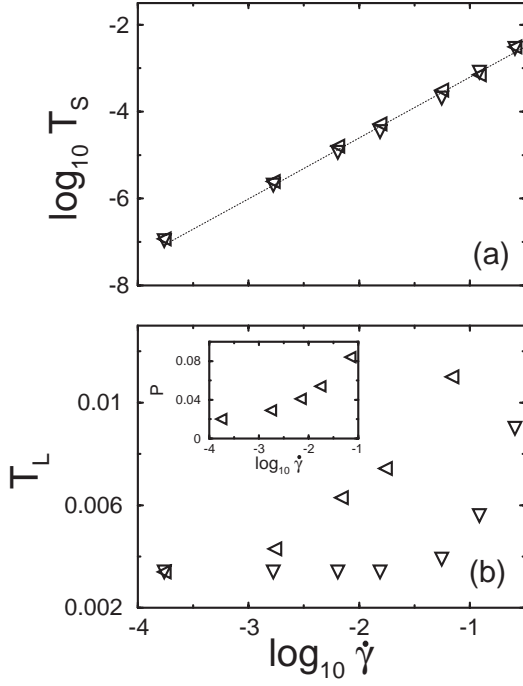


FIG. 2: (a)  $T_S$  and (b)  $T_L$  vs.  $\dot{\gamma}$  for 3d systems with RLJ interactions and  $b = 0.5$  sheared at fixed  $P_{ext} = 0.02$  (downward triangles) or fixed volume fraction  $\phi = 0.68$  (leftward triangles). The dotted line in (a) has slope 1.4. The inset to (b) shows the internal pressure  $P$  vs.  $\dot{\gamma}$  at fixed  $\phi = 0.68$ .

The results for  $R(C)$  for  $\rho(\vec{k})$  at constant normal load presented in Fig. 1(a) are intriguing; they suggest that  $T_L$  is fixed by the pressure in slowly sheared systems. To investigate this question further, we compare  $T_S$  and  $T_L$  in systems sheared at constant normal load (CN) and constant volume fraction (CV) in Fig. 2. We find that  $T_S$  is insensitive to the choice of the ensemble;  $T_S$  scales as a power-law in  $\dot{\gamma}$  over three decades in both ensembles. However, the  $\dot{\gamma}$  dependence of  $T_L$  at CN and CV differs significantly.  $T_L$  in the two ensembles were initially matched at  $\dot{\gamma} \approx 10^{-4}$  and  $P_{ext} = 0.02$  by setting  $\phi$  in the CV simulation equal to  $\langle \phi \rangle$  from the simulation at fixed  $P_{ext} = 0.02$ . At fixed  $\phi$ ,  $T_L$  increases by more than a factor of 3 over the range of  $\dot{\gamma}$  studied. The inset to Fig. 2 (b) suggests that the steady rise in  $T_L$  is due to the shear-induced increase in the internal pressure  $P$  at CV. In contrast,  $T_L$  at fixed  $P_{ext} = 0.02$  remains *constant* over the same range of  $\dot{\gamma}$ .  $T_L$  only begins to increase when  $\dot{\gamma} > \dot{\gamma}_c$ , which in this case is at least 3 decades above the quasi-static  $\dot{\gamma}$  regime at CV.

To test the generality of these results, we performed measurements of  $R(C)$  for  $\rho(\vec{k})$  at two values of the damping constant ( $b = 0.5$  and  $0.04$ ), over a range of normal loads from  $P_{ext} = 0.02$  to 10, and over 4 decades in shear rate [23]. The results are summarized in Fig. 3. Panel (a) shows that for each  $P_{ext}$ , there is a wide range of  $\dot{\gamma}$  over which  $T_L = T_L^0$  is constant.  $T_L$  begins to increase above a characteristic shear rate  $\dot{\gamma}_c$ , which decreases with normal load. Fig. 3 (b) shows that  $T_L$  begins to deviate from  $T_L^0$  as  $T_S$  increases. In this regime, large velocity

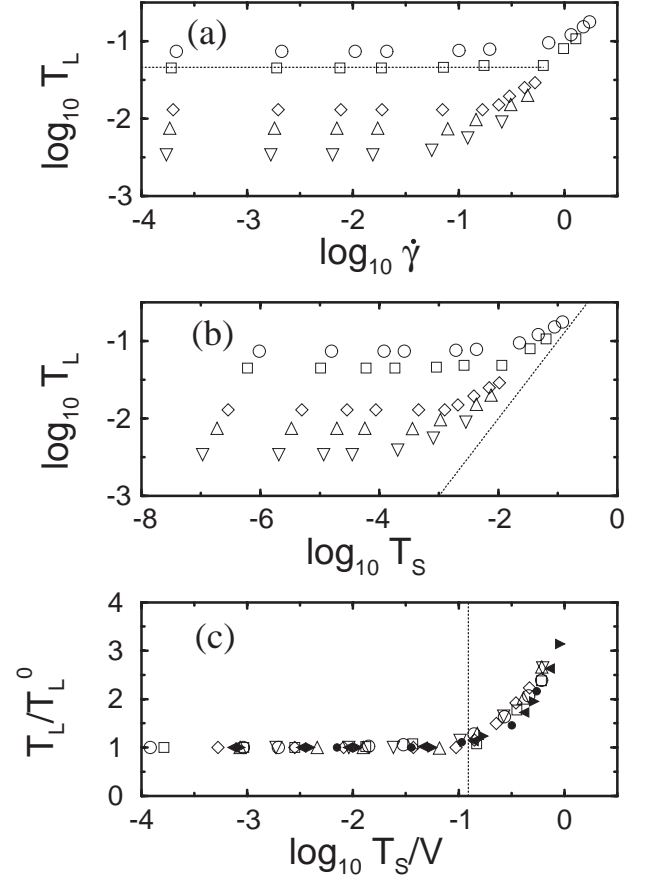


FIG. 3:  $T_L$  plotted vs. (a)  $\dot{\gamma}$  and (b)  $T_S$ . Panel (c) shows  $T_L/T_L^0$  vs. the ratio of  $T_S$  to the total potential energy per particle  $V$ . The results were obtained from 3d systems with RLJ interactions at fixed  $P_{ext}$ . Five loads  $P_{ext} = 0.02$  (downward triangles), 0.05 (upward triangles), 0.1 (diamonds), 0.5 (squares), and 1 (circles) and three loads  $P_{ext} = 2$  (rightward triangles), 5 (leftward triangles), and 10 (small circles) were studied at  $b = 0.5$  (open symbols) and  $0.04$  (filled symbols), respectively. In panel (a), the dotted line defines the low shear rate value  $T_L^0$  of the long-time effective temperature at  $P_{ext} = 0.5$ . In panel (b),  $T_L = T_S$  is indicated by the dotted line. In panel (c), the dotted line marks the ratio of kinetic to potential energy above which  $T_L/T_L^0$  begins to increase for these systems.

fluctuations give rise to frequent rearrangement events and particle diffusion. At each  $P_{ext}$ , there is a  $T_S$  (or  $\dot{\gamma}$ ) regime where sheared athermal systems behave as quasi-equilibrium systems with response proportional to correlation at all times and a single effective temperature  $T_S \approx T_L$  that increases with shear rate. This nontrivial result is not found in sheared glasses because they are thermostatted with  $T_S$  below the glass transition temperature and remain arbitrarily far from equilibrium as the shear rate is tuned.

We seek a general criterion to determine whether sheared athermal systems exist in the pressure-controlled or quasi-equilibrium regime. As a first step, we consider the ratio  $\beta$  of the granular temperature  $T_S$  to the total potential energy per particle  $V$ . For each value of  $b$ , we find that there is a range of normal loads  $P_{ext} > P_{ext}^c$

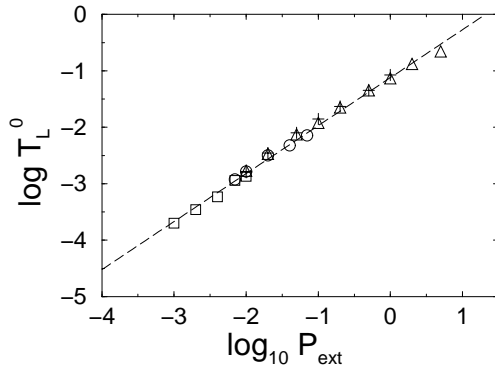


FIG. 4:  $T_L^0$  vs.  $P_{ext}$  for several sheared athermal systems at  $b = 0.5$ : 3d RLJ (triangles), 2d RLJ (pluses), 3d linear spring (circles), and 3d Hertzian spring (squares). The dashed line has slope 0.85.  $P_{ext} > 10^{-1}$  ( $10^{-2}$ ) were not considered for linear (Hertzian) springs because they caused unphysical overlaps.

where  $T_L/T_L^0$  versus  $T_S/V$  is independent of  $P_{ext}$ , with  $P_{ext}^c$  increasing inversely with  $b$ . Fig. 3 (c) shows that when  $P_{ext} > P_{ext}^c$ , there is a characteristic ratio  $\beta_c \approx 0.1$  independent of damping that separates the pressure-controlled and quasi-equilibrium regimes. These results also imply that  $T_L$  in sheared glasses is controlled by pressure since they have  $T_S/V \ll 1$ . The behavior at large  $T_S/V$  in the low-pressure regime  $P_{ext} < P_{ext}^c$  is more complex and will be discussed elsewhere [25].

In Fig. 4 we plot the long-time effective temperature  $T_L^0$  in the pressure-controlled regime vs.  $P_{ext}$  for sheared athermal systems in 2d and 3d with repulsive linear and Hertzian spring and Lennard-Jones interactions. All of

the data collapse onto a power-law with exponent  $0.85 \pm 0.02$ . If both the normal load [24] and  $T_L^0$  scaled linearly with the yield stress of the material, the exponent in Fig. 4 would be 1. Our preliminary results indicate that the yield stress and pressure are proportional [25], which implies that  $T_L^0$  scales sublinearly with the yield stress.

We used MD simulations to study properties of the effective temperature  $T_L$  defined from FD relations for density in athermal systems sheared at fixed normal load. These systems possess two distinct regimes as a function of the ratio  $T_S/V$  of kinetic to potential energy. At small ratios, these systems are pressure-controlled and  $T_L$  is set by the normal load. At large  $T_S/V$ , they behave as quasi-equilibrium systems with  $T_L \approx T_S$  that increases with shear rate. These results point out several difficulties in using  $T_L$  in thermodynamic descriptions of slowly sheared athermal systems. First, the variables  $T_L$ , pressure, and density alone do not provide a complete description of these systems since  $T_L$  and pressure can remain constant while density can vary substantially. Also, these results suggest that when two slowly sheared, athermal systems are placed in contact but maintained at different pressures,  $T_L$  in the two systems will not equilibrate. Thus, in this regime  $T_L$  does not behave as a true temperature variable. We are currently attempting to identify a set of variables that can be used in a thermodynamic description of dense granular shear flows.

We thank R. Behringer, L. Kondic, and A. Liu for helpful comments. Financial support from NASA grant NAG3-2377 (NX) and Yale University (NX,CSO) is gratefully acknowledged.

- 
- [1] J. Casas-Vazquez and D. Jou, *Rep. Prog. Phys.* **66**, 1937 (2003).
  - [2] J. T. Jenkins and M. W. Richman, *Phys. Fluids* **28**, 3485 (1985).
  - [3] S. F. Edwards and R. B. S. Oakeshott, *Physica A* **157**, 1080 (1989).
  - [4] A. Coniglio, F. Fierro, M. Nicodemi, *Physica A* **302**, 193 (2001).
  - [5] L. F. Cugliandolo, J. Kurchan, and L. Peliti, *Phys. Rev. E* **55**, 3898 (1997).
  - [6] J.-L. Barrat and W. Kob, *Europhys. Lett.* **46**, 637 (1999).
  - [7] R. Di Leonardo, L. Angelani, G. Parisi, and G. Ruocco, *Phys. Rev. Lett.* **84**, 6054 (2000).
  - [8] L. Berthier and J.-L. Barrat, *J. Chem. Phys.* **116**, 6228 (2002).
  - [9] C. S. O'Hern, A. J. Liu, and S. R. Nagel, unpublished (cond-mat/0401105).
  - [10] V. Colizza, A. Barrat, and V. Loreto, *Phys. Rev. E* **65**, 050301 (2002).
  - [11] A. Coniglio and M. Nicodemi, *J. Phys.: Condens. Matter* **12**, 6601 (2000).
  - [12] H. A. Makse and J. Kurchan, *Nature* **415**, 614 (2002).
  - [13] L. Kondic and R. P. Behringer, *Europhys. Lett.* **67**, 205 (2004).
  - [14] I. K. Ono, C. S. O'Hern, D. J. Durian, S. A. Langer, A. J. Liu, and S. R. Nagel, *Phys. Rev. Lett.* **89**, 095703 (2002).
  - [15] R. M. Nedderman, *Statics and Kinematics of Granular Materials*, (Cambridge University Press, Cambridge, 1992).
  - [16] P. A. Thompson and G. S. Grest, *Phys. Rev. Lett.* **67**, 1751 (1991).
  - [17] R. Yamamoto and A. Onuki, *Phys. Rev. E* **58**, 3515 (1998).
  - [18] L. E. Silbert, D. Ertas, G. S. Grest, T. C. Halsey, and D. Levine, *Phys. Rev. E* **65**, 031304 (2002).
  - [19] S. Luding, *Phys. Rev. E* **55**, 4720 (1994).
  - [20] M. P. Allen and D. J. Tildesley, *Computer Simulations of Liquids*, (Oxford University Press, Oxford, 1987).
  - [21] N. Xu, C. S. O'Hern, and L. Kondic, unpublished (cond-mat/0403046).
  - [22] Large particles that were less than one large particle diameter from the boundaries were not included in Eq. 5 to avoid boundary effects; thus,  $N_L < N/2$ .
  - [23] At each  $\dot{\gamma}$  and  $P_{ext}$ , we verified that the response was in the linear regime and averaged over at least 500 independent configurations. We also calculated the response and correlation functions at two system sizes,  $N = 256$  and 1024, to show that finite-size effects were small.
  - [24] G. He and M. O. Robbins, *Tribol. Lett.* **10**, 7 (2001).
  - [25] N. Xu and C. S. O'Hern, unpublished.